Mol. Cryst. Liq. Cryst., Vol. 488, pp. 148–162, 2008

ISSN: 1542-1406 print/1563-5287 online
DOI: 10.1080/15421400802240524

Taylor & Francis
Taylor & Francis Group

Generation of Helical Modes of Light by Spin-to-Orbital Angular Momentum Conversion in Inhomogeneous Liquid Crystals

Lorenzo Marrucci
Dipartimento di Scienze Fisiche, Università di Napoli "Federico II", and CNR-INFM "COHERENTIA", Complesso di Monte S. Angelo, Napoli, Italy

The helical modes of an electromagnetic wave are characterized by a helical shape of the wavefront. They carry quantized angular momentum of an orbital kind, as opposed to the spin-like angular momentum that can be associated with circularly polarized waves. Here, I review recent results on a novel method for generating helical waves of light by letting a circularly-polarized non-helical wave pass through an azimuthally inhomogeneous birefringent plate made of a suitably patterned liquid crystal, a device dubbed "q-plate". The q-plate converts the variation of spin angular momentum associated with the switching of light polarization handedness into orbital angular momentum, an optical process that had not been envisioned before.

Generalizing this idea, patterned birefringent plates similar to q-plates may be used for shaping the optical wavefront of a circularly polarized beam in any prescribed way. Moreover, these plates allow fast switching between conjugate wavefronts by inverting the handedness of the input polarization. Devices based on this principle have been called Pancharatnam-Berry phase optical elements.

Keywords: helical modes; liquid crystals; optical elements; orbital angular momentum; Pancharatnam-Berry phase; wavefront shaping

INTRODUCTION

As optical materials, liquid crystals (LC) single, most interesting property is the easiness with which its molecules can be "rotated" by

I thank Domenico Paparo and Carlo Manzo for their contribution to the experimental demonstrations reviewed in this paper.

Address correspondence to Lorenzo Marrucci, Dipartimento di Scienze Fisiche, Università di Napoli "Federico II", and CNR-INFM "COHERENTIA", Complesso di Monte S. Angelo, via Cintia, 80126 Napoli, Italy. E-mail: lorenzo.marrucci@na.infn.it

the action of external fields. Electric and magnetic fields in particular may rotate the molecules of LCs, thus changing the medium optical properties and affecting the transmitted light. The electric field of the light itself can also induce a rotation of the LC molecules, thus giving rise to all sorts of strongly nonlinear optical phenomena [1]. This capability of light of "spinning" the LC molecules has been technically described in terms of the transfer of angular momentum from light to matter [2–4]. This transfer is possible for all sorts of materials, but liquid crystals are among the most effective ones in coupling to the angular momentum of light.

Thus far, however, the attention has been focused on the possibility of using light for rotating the LC molecules (or eventually whole LC droplets [5]). In this paper, I consider instead the reverse point of view: using LCs for inducing a "rotation" of a light beam. We will see that novel optical phenomena are actually possible that hitherto had not been envisioned. But before introducing these phenomena, I must first clarify the concept of a "rotating" light beam.

It is well known that a light beam can carry angular momentum oriented along the beam itself. In layman words, this corresponds to saying that the light beam may "rotate upon itself", while propagating. However, less well known is the fact that there actually are two different ways for the beam to rotate, or to carry angular momentum. The first, more widely known, way is the "spin-like" form of angular momentum, associated with the optical polarization. A circularly polarized beam of light is composed of photons carrying each one unit of $\hbar$ of "spin" angular momentum, directed forward along the beam in the case of left-handed polarization, and backward in the case of right-handed one. The second way is the so-called "orbital" form of the angular momentum, that is associated with the possibility of having a helical shape of the beam wavefront [6]. Adopting cylindrical coordinates r, ϕ, z with the beam axis coincident with the z axis, the mathematical expression of the optical electric field in a generic helical wave is the following (in the paraxial approximation):

$$\mathbf{E}(r, \varphi, z, t) = \mathbf{E}_0(r, z) e^{im\varphi} e^{i(kz - \omega t)} \tag{1}$$

where ω is the wave (angular) frequency, $k = 2\pi/\lambda$ is the wavenumber, with λ the wavelength, and m is an integer characterizing the "degree and sign of the helicity". The wavefront shape of these helical modes is shown in Figure 1. For $m \neq 0$, a helical mode must have an optical vortex at the beam center, where the phase is undefined. Most importantly, these waves are composed of photons carrying $|m|\hbar$ units of "orbital" angular momentum each, directed forward or backward

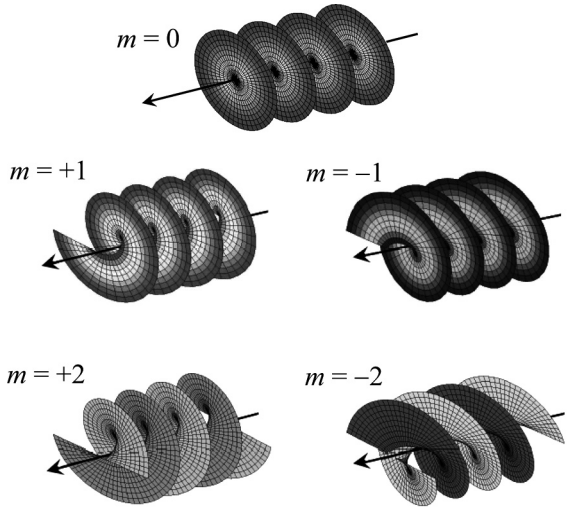

FIGURE 1 Examples of helical waves. Represented is the wavefront shape of helical modes, for helicities $m = 0$ (plane wave), $m = \pm 1$ and $m = \pm 2$.

along the beam according to the handedness of the wavefront helix or to the sign of m. For certain specific choices of the radial profile $\mathbf{E}_0(r)$ at a given plane z, Eq. (1) will correspond to a Laguerre-Gaussian mode [7]. It must be emphasized that this angular momentum, although labelled "orbital", is still an "internal" kind of angular momentum according to the standard mechanical definition, i.e. its value is fully independent of the choice of the origin [8].

The optical "rotation" of the beam can be revealed by the interaction of light with matter. For example, by letting a beam carrying angular momentum impinge on a small optically-absorbing particle, the latter will be set in rotation by the action of light. If the particle is located at the beam axis, spin and orbital angular momentum of light will both induce the same effect, with the particle starting to rotate around its center of mass, i.e., acquiring "internal" angular momentum from light. In contrast, when the particle is located off the beam axis, the spin angular momentum of light will still "transfer" into the internal angular momentum of the particle, but the orbital angular momentum will instead induce a revolution of the particle around the beam axis, i.e., it will be transferred to the external angular momentum of the particle.

Absorption of light gives rise to a one-way exchange of angular momentum between light and matter: the photon angular momentum

is entirely transferred to the material medium. Two-way exchange of angular momentum may instead occur in transparent media. Two simpler limit cases have been throughly investigated in the past: (i) anisotropic homogeneous media, such as birefringent crystals or wave plates, which couple effectively only with the spin form of optical angular momentum; (ii) inhomogeneous isotropic media, which couple effectively only with the orbital form of optical angular momentum. Since a short time ago, it remained entirely unexplored the case of transparent media which can be at the same time strongly optically anisotropic (birefringent) and inhomogeneous. LCs are clearly an outstanding example of materials having both these properties. Although many works have been published in the past on the coupling between the angular momentum of light and LCs, most of them focused only on the exchange of the spin form of angular momentum (e.g., [2–4]), neglecting the role of inhomogeneity and of the exchange of orbital angular momentum. More recent works have considered also the exchange of orbital angular momentum, but still with an emphasis on the induced LC dynamics, i.e. still "light rotating LC molecules" and not the reverse [9]. Then, after a first theoretical paper considering the problem only from a strictly formal point of view [10], came the experimental work which is reviewed here [11,12]: the possibility of using suitably patterned LC devices for coupling the spin and orbital angular momenta of light with each other ("spin-to-orbital angular momentum conversion" [11]), and thus for generating helical modes of light in a new way, allowing fast switching between several different values of the orbital angular momentum [12]. This corresponds to saying the LCs have been used, for the first time, for "rotating" a light beam.

A NOVEL LIQUID CRYSTAL OPTICAL DEVICE: THE *q*-PLATE

Let us consider a planar LC cell having a thickness and material birefringence chosen so as to induce a homogeneous phase retardation of $\delta = \pi$ (corresponding to half-wave), at the working wavelength λ, for light propagation perpendicular to the cell plane walls (z axis). The LC molecular director $\mathbf{n}$ is assumed to be uniform in the z direction, but inhomogeneous in the xy plane of the cell, according to a prescribed pattern $\mathbf{n}(x,y) = \mathbf{n}(r,\phi)$.

Neglecting all transverse diffraction effects occurring in the propagation within the plate, one can use the Jones formalism to fully characterize the optical propagation through the plate. Let $\alpha(x,y)$ be the angle between $\mathbf{n}(x,y)$ and a fixed reference axis x. The Jones matrix $\mathbf{M}$ describing the cell action on the field at each transverse position

x, y is the following:

$$\mathbf{M}(x,y) = \begin{bmatrix} \cos 2\alpha(x,y) & \sin 2\alpha(x,y) \\ \sin 2\alpha(x,y) & -\cos 2\alpha(x,y) \end{bmatrix} \tag{2}$$

An input circularly polarized plane wave, described by the Jones electric-field vector

$$\mathbf{E}_{in}(x,y) = E_0 \begin{bmatrix} 1 \\ \pm i \end{bmatrix} \tag{3}$$

(where the $\pm$ is $+$ for the left-circular case and $-$ for the right-circular one), will be transformed by the action of the cell into the following field (up to an overall phase):

$$\mathbf{E}_{out}(x,y) = \mathbf{M}(x,y)\mathbf{E}_{in}(x,y) = E_0 e^{\pm i2\alpha(x,y)} \begin{bmatrix} 1 \\ \mp i \end{bmatrix} \tag{4}$$

It is seen from this equation that the output wave is still circularly polarized, but with the opposite polarization handedness. This is expected, as any half-wave plate inverts the handedness of circular polarization. More interestingly, the output field wavefront has acquired a nonuniform phase retardation

$$\Delta\Phi(x,y) = \pm 2\alpha(x,y) \tag{5}$$

This result is very general: any wavefront shape as specified by the transverse phase retardation $\Delta\Phi(x,y)$, can be generated by a suitable pattern of the LC cell. The needed director geometry is fixed by Eq. (5), where the sign is determined by the circular polarization handedness that will be employed. The same device will also generate the conjugate wavefront $-\Delta\Phi(x,y)$ if the input polarization handedness is inverted. This particular approach to optical wavefront shaping is related with the so-called Pancharatnam-Berry geometric phase [13,14]. Wavefront-shaping devices based on this principle have been realized only recently and have been named "Pancharatnam-Berry phase optical elements" (PBOE) [12,15,16].

Let us now consider a specific pattern geometry, given by the following law:

$$\alpha(r,\varphi) = \alpha_0 + q\varphi \tag{6}$$

where α_0 and q and are constants. Note that Eq. (6) implies the presence of a topological liquid crystal defect in the medium localized at the cell center, i.e., $r = 0$. However, if q is an integer or a semi-integer there will be no discontinuity line in the cell. In the following, we will refer to LC cells having the above specified geometry as q-plates

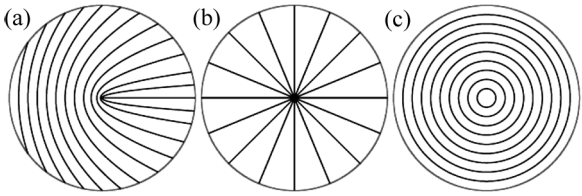

FIGURE 2 Examples of q-plates. The tangent to the lines shown indicate the local direction of the optical axis (molecular director) $\mathbf{n}$. (a) $q = 1/2$ and $\alpha_0 = 0$ (a nonzero α_0 is here just equivalent to an overall rigid rotation), which generates helical modes with $m = \pm 1$; (b) $q = 1$ with $\alpha_0 = 0$ and (c) with $\alpha_0 = \pi/2$, which can be both used to generate modes with $m = \pm 2$.

(i.e., q-plates form a subclass of PBOEs). A few examples of q-plate geometries for different values of q and α_0 are shown in Figure 2.

Inserting Eq. (6) in Eq. (4) (or Eq. (5)), we obtain the field (or its wavefront phase) generated by a q-plate for the case of a circularly polarized input plane-wave. Apart from an irrelevant overall phase, the outgoing wave field (for any plane z and time t) is given by the following expression:

$$\mathbf{E}_{out}(x,y) = E_0 e^{\pm i2q\varphi \pm i2\alpha_0} \begin{bmatrix} 1 \\ \mp i \end{bmatrix} \tag{7}$$

Comparing this expression with that given in Eq. (1) we see that this output field corresponds to a helical mode with helicity number

$$m = \pm 2q \tag{8}$$

In other words the output wavefront is helical and the sign of the helicity is controlled by the input polarization handedness. The helicity magnitude $|m|$ is instead fixed by the LC cell geometry, via its characteristic integer or semi-integer parameter q.

It should be noted here that the $q = 1$ geometry presents an important particular property: it is rotationally symmetric around the coordinate origin. This special case will be discussed in further detail in the next section.

Before moving on, however, let us briefly discuss what happens if the birefringent phase retardation δ across the LC q-plate is not exactly half-wave (i.e., $\delta \neq \pi$). In that case, the Jones matrix given in Eq. (2) must be replaced with the following one:

$$\mathbf{M}(x,y) = \cos\frac{\delta}{2}\begin{bmatrix} 1 & 0 \\ 0 & 1 \end{bmatrix} + i\sin\frac{\delta}{2}\begin{bmatrix} \cos 2\alpha(x,y) & \sin 2\alpha(x,y) \\ \sin 2\alpha(x,y) & -\cos 2\alpha(x,y) \end{bmatrix} \tag{9}$$

When this matrix is applied to the input field given by Eq. (3), we obtain the following output:

$$\mathbf{E}_{out}(x,y) = E_0 \cos\frac{\delta}{2}\begin{bmatrix}1\\ \pm i\end{bmatrix} + iE_0 \sin\frac{\delta}{2} e^{\pm i2q\varphi \pm i2\alpha_0}\begin{bmatrix}1\\ \mp i\end{bmatrix} \tag{10}$$

corresponding to a *coherent* superposition of a plane-wave field that has the same circular polarization as the input one and of a helical field having reversed circular polarization. The relative amplitudes of these two components of the output field are fixed by δ.

SPIN-TO-ORBITAL ANGULAR MOMENTUM CONVERSION

Let us consider the angular momentum balance for a single photon passing through a q-plate (with $\delta = \pi$, for the time being). Let us assume that the input photon polarization is left-circular and its wavefront is plane. Then its spin angular momentum (z component) is $+\hbar$, while the orbital angular momentum is zero. The total angular momentum of the photon is equal to the spin one. At the output of the plate, the polarization is right-circular and the wavefront is helical, with $m = 2q$. Therefore the photon spin angular momentum is $-\hbar$, while the orbital angular momentum is $2q\hbar$. The total angular momentum is therefore $(2q-1)\hbar$ and the overall *variation* of angular momentum suffered by the photon in crossing the q-plate is

$$\Delta L_z = (2q-1)\hbar - \hbar = 2(q-1)\hbar \tag{11}$$

Since angular momentum must be conserved, this variation must be exchanged with the medium, i.e. with the q-plate. Multiplied by the photon flux, it leads to a total torque on the medium given by

$$M_z = -\Delta L_z \frac{P}{\hbar\omega} = 2(1-q)\frac{P}{\omega} \tag{12}$$

where P is the beam optical power and all reflections (or other losses) have been neglected.

A similar transformation occurs also if the input photon is not in a plane wave but it is instead already in a helical mode carrying orbital angular momentum. In a quantum language, the general photon transformation occurring in the q-plate is given by the following expression:

$$|\psi\rangle_{in} = |\pm 1, m\rangle \xrightarrow{q\text{-plate}} |\psi\rangle_{out} = e^{\pm i2\alpha_0}|\mp 1, m \pm 2q\rangle \tag{13}$$

where the first ± 1 in the ket indicates the spin angular momentum and the second integer indicates the orbital angular momentum, both

in units of $\hbar$ (it must be noted that these two quantum numbers do not completely define the photon state: a "radial" number remains unspecified, but it is unnecessary for our discussion here).

The case $q = 1$ leads to a special result: the photon crossing the q-plate does not change its total angular momentum, and therefore no torque is generated on the medium. However, it must be emphasized that spin and orbital angular momenta of the photon are both varied in the q-plate: the spin switches sign, passing from $+\hbar$ to $-\hbar$, while the orbital angular momentum passes from zero to $2\hbar$. The two variations exactly cancel each other! This phenomenon in which angular momentum of light changes its nature, exploiting the interaction with the medium but remaining entirely within the optical field, was called "*spin-to-orbital angular momentum conversion*" [11]. Most importantly, if the input photon has a right-circular polarization, the two variations are both sign-inverted, thus still giving all-optical angular momentum conservation. This optical process is pictorially illustrated in Figure 3.

The reason why the case $q = 1$ is special is related with its rotational symmetry. It is known, indeed that media which are globally rotationally symmetric around an axis, even if locally anisotropic, cannot exchange angular momentum with light (as long as the coordinate origin is on the symmetry axis).

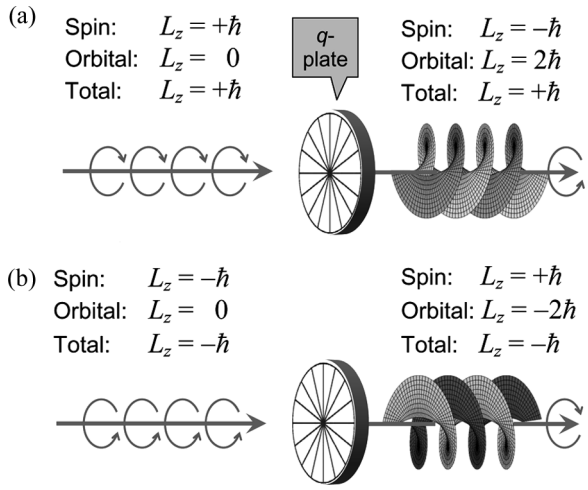

FIGURE 3 Pictorial description of the spin-to-orbital angular momentum conversion occurring in a q-plate with $q = 1$, for a single photon. (a) Left-circular input polarization. (b) Right-circular input polarization.

And indeed, the all-optical angular momentum conservation occurs also in the case in which $\delta \neq \pi$. In this case the q-plate quantum transformation is the following:

$$|\psi\rangle_{in} = |\pm 1, m\rangle \xrightarrow{q\text{-plate}} |\psi\rangle_{out} = \cos\frac{\delta}{2}|\pm 1, m\rangle + i \sin\frac{\delta}{2} e^{\pm i 2\alpha_0} |\mp 1, m \pm 2q\rangle \tag{14}$$

and the final photon quantum state is the superposition of a "unmodified" photon and a "converted" photon. In both states of the superposition the overall photon angular momentum is conserved, although the angular momentum conversion in the photon occurs only with a finite probability, given by $\sin^2(\delta/2)$.

EXPERIMENT

To demonstrate the angular momentum conversion predicted in the previous Section, in the work reported in Refs. [11] and [12], my coworkers and I manufactured LC $q = 1$ plates working at the visible wavelength $\lambda = 633\,\text{nm}$. LC planar cells made with the nematic commercial mixture E63 were prepared so as to obtain a birefringence retardation of approximately a half wave. Details on the cell preparation are reported in Ref. [12]. In particular, the $q = 1$-plate geometry was obtained by a "circular rubbing" procedure, so as to obtain a surface easy axis for the LC director orientation as that shown in Figure 2c. To test the optical effect of the manufactured q-plate, a circularly-polarized He-Ne laser beam having a TEM_{00} transverse mode and a beam-waist radius of about 1 mm was sent through it, taking care of aligning the beam axis on the q-plate center. The intensity profile of the output beam was found to have the "doughnut" shape expected for a helical mode. In order to measure also the wavefront shape of the light emerging from the q-plate, we set up a Mach-Zender interferometer, schematically shown in Figure 4. The signal-arm beam of the interferometer was first circularly polarized with the desired handedness by means of properly oriented quarter-wave plate and then was sent through the LC q-plate. The beam emerging from the q-plate was then sent through another quarter-wave plate and a linear polarizer, arranged for transmitting the polarization handedness opposite to the initial one, so as to eliminate the residual unchanged circular polarization (this step is not necessary when using a q-plate having exactly half-wave retardation). Finally, the signal beam was superimposed with the reference and thus generated an interference pattern on a screen or directly on the sensing area of a CCD camera. Two different interference geometries were

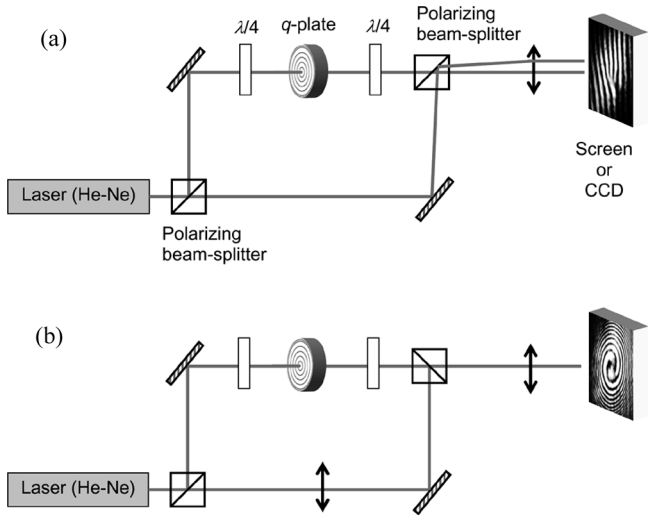

FIGURE 4 Sketch of the Mach-Zender setup employed for proving the generation of helical modes and the corresponding conversion of angular momentum. (a) First layout, with slightly misaligned arms of the interferometer. (b) Second layout, with the reference beam having a different wavefront curvature from the signal beam, as obtained by inserting a lens in its arm.

employed. In the first, shown in Figure 4a, the reference beam wavefront was kept approximately plane (more precisely, it had the same wavefront curvature as the signal beam) but the two beams were slightly tilted with respect to each other. For non-helical waves, this geometry gives rise to a regular pattern of parallel straight fringes. If the wavefront of the signal beam is helical, the pattern develops a dislocation (double, in this case, since $q = 1$ yields $m = \pm 2$), with an orientation depending on the sign of m and the relative orientation of the two beams. In the second geometry, shown in Figure 4b, the reference beam wavefront was approximately spherical, as obtained by inserting a lens in the reference arm. For non-helical waves, the resulting interference pattern is made of concentric circular fringes. If the wavefront of the signal beam is helical, the pattern takes instead the form of a spiral (a double spiral, for $m = \pm 2$), with a handedness depending on the sign of m (counterclockwise outgoing spirals, seen against the propagation direction as in our CCD images, correspond to a positive m). Figure 5 shows the CCD-acquired images of the interference patterns we obtained in the two geometries, respectively for a left-circular [panels (a) and (c)] and right-circular [panels (b) and (d)]

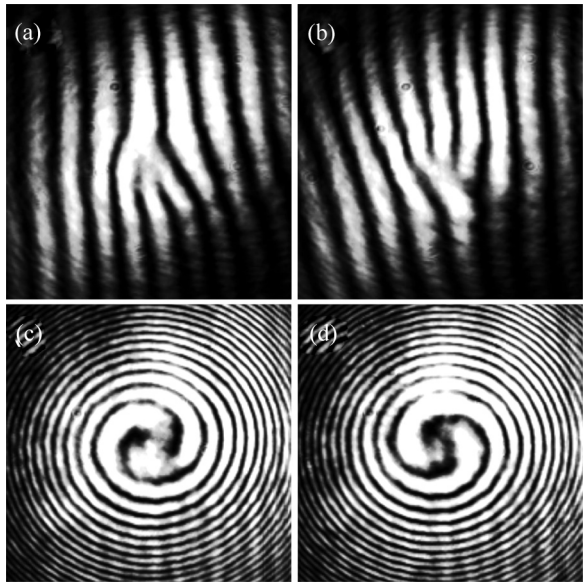

FIGURE 5 Recorded interference patterns generated by the q-plate with $q = 1$. (a–b) panels refer to the first layout (plane-wave reference geometry, see Fig. 4a), (c–d) panels to the second one (spherical-wave reference, see Fig. 4b). Panels on the left, (a) and (c), are for a left-circular input polarization and those on the right, (b) and (d), for a right-circular one.

input polarizations. These results show unambiguously that the wavefront of the light emerging from the q-plate is indeed helical with $m = \pm 2$, as predicted, and that it carries an orbital angular momentum just opposite to the variation of spin angular momentum associated with the polarization occurring in the plate. This demonstrated the spin-to-orbital conversion of optical angular momentum.

PROSPECTS

The LC q-plate that was manufactured for demonstrating the angular momentum conversion is also the first example of a PBOE made with liquid crystals and also the first demonstrated PBOE working in the visible domain.

Its polarization-based control of the generated helical wavefront seen in the previous Section is a good example of the possible general advantages of the peculiar PBOE approach to wavefront shaping. Indeed, all other existing approaches to helical mode generation

(i.e. cylindrical lenses, spiral phase plates, and holographic methods) have an essentially fixed output. Of course, by introducing a suitable spatial light modulator, dynamical control becomes possible, but only at relatively low switching rates. This limitation is particularly important in applications related with optical information encoding, as it severely limits the communication bandwidth. In contrast, in the approach described here, based on q-plates, a simple electro-optical control of the input polarization allows switching of the generated helical mode at very high rate. By cascading several q-plates in series with suitable electro-optic devices in between, one can obtain fast switching among several different helical orders. This could be very useful if helical modes are to be used in multi-state optical information encoding, as recently proposed for classical communication [17] and for quantum communication and computation [18,19].

Although in the proof-of-principle demonstration reviewed here, the employed method for patterning the LC cell works only for circular-symmetric geometries (as in the $q = 1$ plate), LC cell patterning has the potential for obtaining any desired PBOE geometry. Different approaches can be explored, such as micro-rubbing [20], masked or holographic photo-alignment [21,22], and silicon-oxide evaporated coatings [23].

It must be emphasized that, independently of the wavefront shape to be generated, the optical thickness of the LC cell will be uniform. It can also be very thin, if the material is sufficiently birefringent. Nematic LC, that have a typical birefringence $\Delta n \approx 0.2$, if assembled in the planar geometry can yield a half-wave birefringent retardation with a thickness d of about two wavelengths (more precisely, $d = \lambda/(2\Delta n) \approx 2.5\lambda$), i.e. just above a micron for the visible domain. The necessity of having thick containing glasses might be also eliminated by using polymeric free-standing LC films (which could be aligned by photo-alignment techniques). Despite the small thickness, there is no a priori limitation set on the relative phase retardation between different parts of the generated wavefront. Phase retardations of several wavelengths between any two different points of the wavefront can be obtained just by having the director **n** make several complete (2π) rotations along the line connecting the two points in the cell.

As an example of the possible applications of these PBOE phase optical elements made with LC, consider, for example, a hypothetical LC cell having a geometry defined by the radial-quadratic law $\alpha(r, \varphi) = cr^2$ where c is a constant [15,24]. Such a geometry is illustrated in Figure 6. This cell will induce a parabolic phase retardation on the input wave, leading to a focusing or defocusing effect,

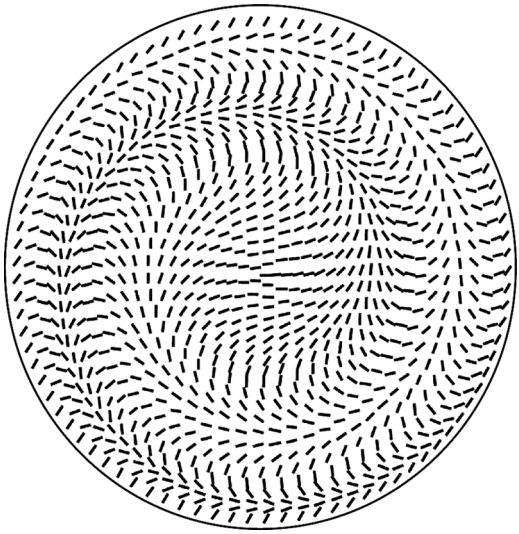

FIGURE 6 Easy axis geometry of a hypothetical liquid crystal planar cell behaving as a (polarization-dependent) PBOE lens. Dashes indicate local director for a selection of radii. A perfect PBOE-lens will actually have a continuous variation of the optical axis.

depending on the retardation sign. In other words, this PBOE will act on a circularly polarized input as a lens having focal length given by $f = \pm\pi/(2c\lambda)$, with the sign depending on the input polarization handedness. As mentioned before, this PBOE-lens will have a uniform thickness, which can be very small. This feature cannot be matched by standard lenses (including GRIN elements) and will likely find some use in certain specific applications. Only Fresnel lenses can have a similar thickness uniformity (on the average), but at the price of introducing several transverse discontinuities of optical properties (either the thickness or the refractive index), thus making the manufacturing difficult and expensive and imposing unwanted optical losses. In contrast, PBOE are perfectly continuous and optical losses can be minimal.

CONCLUSIONS

In this paper I have reviewed some recent results on a new approach to the manipulation of the angular momentum of light, introducing an interaction between the spin and the orbital degrees of freedom of light taking place in liquid crystals. In particular, a specific LC geometry

realizes a perfect all-optical conversion of spin angular momentum into orbital angular momementum, with no net transfer of angular momentum to matter. This allows for the generation of helical modes of light carrying orbital angular momentum, with the possibility of fast electro-optic switching among several helical states.

This approach to the generation of helical modes of light could prove particularly valuable in the foreseen applications of these modes to the multi-state information encoding for classical and quantum communication and computation, where the capability for a fast switching of the generated helicity is critical. Moreover, single-beam quantum computation with spin and orbital angular momentum states becomes possible.

The working principle behind the interaction of optical spin and orbital angular momenta is based on the Pancharatnam-Berry geometrical phase. This principle is at the root of recently-developed optical elements for wavefront shaping that are polarization-controlled. Technologies of patterned liquid crystals and of polarization holography in polymers are available to manufacture these optical elements for the visible domain, with very interesting prospects for a variety of optical applications.

REFERENCES

[1] Marrucci, L. & Shen, Y. R. (1998). In: *The Optics of Thermotropic Liquid Crystals*, Sambles, R. & Elston, S. (Eds.), Taylor & Francis: London, Chapter 6, 115.
[2] Santamato, E., Daino, B., Romagnoli, M., Settembre, M., & Shen, Y. R. (1986). *Phys. Rev. Lett.*, *57*, 2423.
[3] Abbate, G., Maddalena, P., Marrucci, L., Saetta, L., & Santamato, E. (1991). *Phys. Scripta*, *T39*, 389.
[4] Marrucci, L., Abbate, G., Ferraiuolo, S., Maddalena, P., & Santamato, E. (1992). *Phys. Rev. A*, *46*, 4859.
[5] Manzo, C., Paparo, D., Marrucci, L., & Jánossy, I. (2006). *Phys. Rev. E*, *73*, 051707.
[6] Padgett, M. J., Courtial, J., & Allen, L. (2004). *Phys. Today*, *57*(5), 35.
[7] Allen, L., Beijersbergen, M. W., Spreeuw, R. J. C., & Woerdman, J. P. (1992). *Phys. Rev. A*, *45*, 8185.
[8] O'Neil, A. T., MacVicar, I., Allen, L., & Padgett, M. J. (2002). *Phys. Rev. Lett.*, *88*, 053601.
[9] Piccirillo, B., Toscano, C., Vetrano, F., & Santamato, E. (2001). *Phys. Rev. Lett.*, *86*, 2285.
[10] Piccirillo, B. & Santamato, E. (2004). *Phys. Rev. E*, *69*, 056613.
[11] Marrucci, L., Manzo, C., & Paparo, D. (2006). *Phys. Rev. Lett.*, *96*, 163905.
[12] Marrucci, L., Manzo, C., & Paparo, D. (2006). *Appl. Phys. Lett.*, *88*, 221102.
[13] Pancharatnam, S. (1956). *Proc. Indian Acad. Sci. Sect. A*, *44*, 247.
[14] Berry, M. V. (1987). *J. Mod. Opt.*, *34*, 1401.
[15] Bhandari, R. (1997). *Phys. Rep.*, *281*, 1.
[16] Bomzon, Z., Biener, G., Kleiner, V., & Hasman, E. (2002). *Opt. Lett.*, *27*, 1141.

[17] Gibson, G., Courtial, J., Padgett, M. J., Vasnetsov, M., Pas'ko, V., Barnett, S. M., & Franke-Arnold, S. (2004). *Opt. Express*, *12*, 5448.
[18] Leach, J., Padgett, M. J., Barnett, S. M., Franke-Arnold, S., & Courtial, J. (2002). *Phys. Rev. Lett.*, *88*, 257901.
[19] Vaziri, A., Weihs, G., & Zeilinger, A. (2002). *Phys. Rev. Lett.*, *89*, 240401.
[20] Varghese, S., Crawford, G. P., Bastiaansen, C. W. M., de Boer, D. K. G., & Broer, D. J. (2004). *Appl. Phys. Lett.*, **85**, 230.
[21] Schadt, M., Seiberle, H., & Schuster, A. (1996). *Nature*, *381*, 212.
[22] Fan, Y.-H., Ren, H., & Wu, S.-T. (2003). *Opt. Express*, *11*, 3080.
[23] Chen, J., Bos, P. J., Bryant, D. R., Johnson, D. L., Jamal, S. H., & Kelly, J. R. (1995). *Appl. Phys. Lett.*, *67*, 1990.
[24] Hasman, E., Kleiner, V., Biener, G., & Niv, A. (2003). *Appl. Phys. Lett.*, *82*, 328.